Dalton Transactions

ROYAL SOCIETY OF CHEMISTRY

PERSPECTIVE

View Article Online
View Journal | View Issue

Cite this: *Dalton Trans.*, 2023, **52**, 9189

Amidoboronates: bringing together the synthesis of BN-heterocycles *via* a reductive coupling and dynamic covalent chemistry

Anna J. McConnell [a,b]

Received 15th June 2023,
Accepted 19th June 2023

DOI: 10.1039/d3dt01863f

rsc.li/dalton

This Perspective describes how amidoboronates open up new chemical space spanning the areas of BN-heterocycles and dynamic covalent chemistry. BN-containing heterocycles offer the potential to access new properties and reactivity compared to their C–C analogues. Amidoboronates are introduced as a new class of B–N heterocycles that can be synthesised in three isomeric forms (*meso*$_5$, *rac*$_5$ and *rac*$_6$) from the reductive coupling of *N*-aryl iminoboronates. Furthermore, initial investigations on the dynamic covalent chemistry of amidoboronates are discussed, such as the reversibility of C–C bond formation following the reductive coupling and tuning the *rac*$_5$/*rac*$_6$ ratio *via* dynamic covalent B–N and B–O bonds.

Introduction

Given the isoelectronic nature of CC and BN bonds (Fig. 1a), BN-containing heterocycles[1–14] have been investigated as CC isosteres. However, the polarity of the B–N bond alters the electronic properties, leading to different reactivity and selectivity compared to their carbon analogues.[9,11] Furthermore, B–N bonds can take the form of coordinative or covalent bonds (Fig. 1a), offering additional avenues for accessing new types of chemistry and tuning properties. As a result, BN-heterocycles, such as azaborines, BN-naphthalenes and BN-polyaromatic hydrocarbons (PAHs), have been exploited in applications from materials science as BN-doped nanographenes[10] to catalysis.[12]

Despite the interest in BN-heterocycles, methods for their synthesis (particularly in the quantities required for applications) are still limited compared with the myriad of synthetic methods available in organic chemistry for the synthesis of CC analogues.[7,8] Thus, synthetic access to BN-heterocycles is limiting their diversity and the exploration of new chemical space,[7] for example in the context of dynamic covalent chemistry.

Dynamic covalent chemistry combines the strength of covalent bonds with the reversibility of bond formation, enabling for example the self-assembly of supramolecular architectures from mechanically interlocked molecules to cages from smaller building blocks under thermodynamic control.[15–19] While the dynamic covalent chemistry of a variety of bonds including S–S,[16,20–22] C=C,[23,24] C=N,[22,24–28] C–O,[17,29] Si–O[30,31] and B–O[19,22,32–34] bonds has been established, the discovery of new types of dynamic covalent bonds, *e.g.* based on B–N bonds, could open up new avenues for applications.

This Perspective highlights how these two research fields, B–N heterocycles and dynamic covalent chemistry, have intersected through the synthesis of amidoboronates **3–4** (Fig. 1b), a new class of BN-heterocycles, and established new research directions. A family of amidoboronates has been prepared *via* the reductive coupling of *N*-aryl iminoboronates **1** with reduced synthetic effort exploiting the modular synthesis of the iminoboronate substrates and the formation of up to three isomeric amidoboronate products (*meso*$_5$, *rac*$_5$ and *rac*$_6$).

[a]*Otto Diels Institute of Organic Chemistry, Kiel University, Otto-Hahn-Platz 4, Kiel 24098, Germany*
[b]*Department of Chemistry and Biology, University of Siegen, Adolf-Reichwein-Strasse 2, 57068 Siegen, Germany. E-mail: anna.mcconnell@uni-siegen.de*

Anna J. McConnell

Anna McConnell obtained a D.Phil. under the supervision of Prof. Paul Beer from the University of Oxford. She completed postdoctoral research stays in the group of Prof. Jacqueline Barton at the California Institute of Technology and at the University of Cambridge with Prof. Jonathan Nitschke. From 2016–2023 she was a Junior Professor at Christian-Albrechts-Universität zu Kiel and in 2023 she joined the University of Siegen as a Junior Professor. Her research focuses on stimuli-responsive metal–organic cages, dynamic covalent chemistry and luminescent complexes.

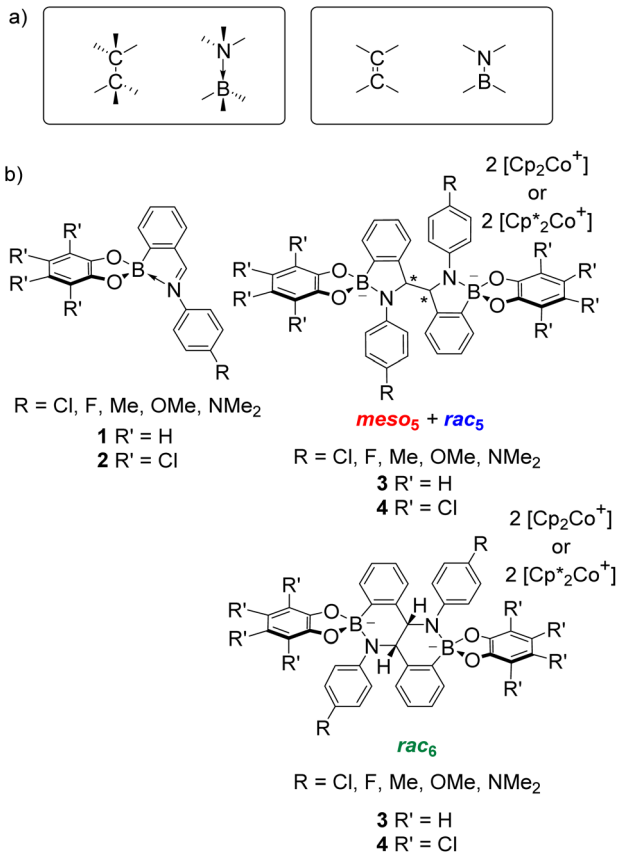

Fig. 1 (a) Isoelectronic relationship between CC and BN bonds. (b) Iminoboronates **1–2** for the synthesis of amidoboronates **3–4** *via* a reductive coupling.

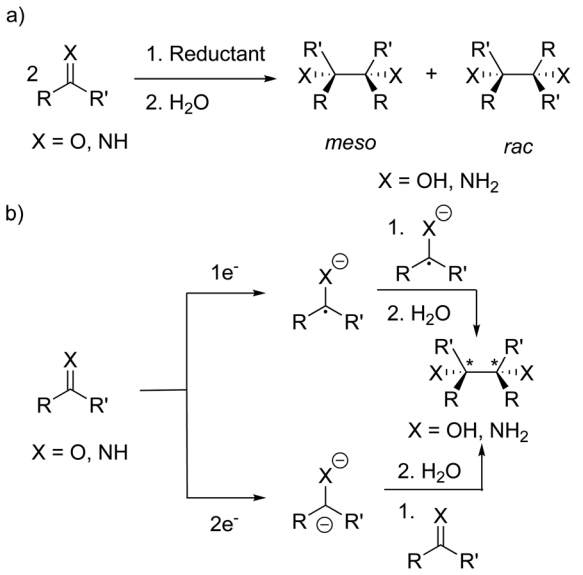

Scheme 1 (a) Reductive coupling of aldehydes, ketones and imines giving 1,2-diols and 1,2-diamines, respectively, as a mixture of *meso* and *rac* diastereomers. (b) Two proposed mechanisms for the reductive couplings: one electron reduction to the radical anion and recombination of two radical anions; two electron reduction to the dianion and reaction with a second aldehyde/ketone/imine.

Furthermore, the dynamic covalent chemistry of the amidoboronates including the rearrangement between the rac_5 and rac_6 isomers *via* dynamic covalent B–N bonds is discussed.

C–C bond formation *via* reductive couplings

Synthesis of 1,2-diamines and 1,2-diols

Radical-mediated reductive couplings such as the pinacol coupling have been exploited in organic chemistry to form C–C bonds, giving access to 1,2-diamines[35–44] and 1,2-diols[39,42–52] *via* the reductive coupling of imines and carbonyl compounds, respectively (Scheme 1a). A variety of metal-based reagents including alkali metals,[35–37] Mg(I) compounds,[53] "GaI",[41] SmI_2[38] and Mn*[39] have been used as the stoichiometric reductant. More recently, metal-free reductive couplings[45,48,49] have been reported and replacement of the stoichiometric reductant with a photocatalyst has led to the development of photoredox-catalysed reductive couplings.[42–44,46,47,50,52]

Several mechanisms have been proposed for the reductive couplings (Scheme 1b): (a) one electron reduction forming a radical anion and the formation of the dimer *via* coupling of two radical anions; (b) two electron reduction to the dianion and disproportionation upon reaction with a second C=O/C=N molecule.[35,37] Furthermore, the dimers can form as a mixture of *meso* and *rac* diastereomers since the newly formed C–C bond contains two stereogenic centres (when R ≠ R′); in separate studies, Eisch[35] and Smith[36] investigated the influence of the reaction conditions (*e.g.* solvent and reductant) on the ratio of the *meso* and *rac* diastereomers. In some cases (*e.g.* with sodium or potassium in THF), only the *rac* isomer was observed and isomerisation of the initially formed diasteromeric mixture to the *rac* isomer was hypothesised.[35,36] Eisch and co-workers proposed ion-pairing between the radical anion and countercation favours *rac* isomer formation,[35] whereas Smith and co-workers proposed a radical anion/dimeric dianion equilibrium where the *rac* diastereomer is the thermodynamic product of the reaction.[36,37]

Synthesis of B–N heterocyclic dimers

Reductive couplings have also been exploited to access BN-heterocyclic dimers following C–C bond formation (Schemes 2 and 3).[3,6] Given the electron-deficiency of boron, the reactivity of the boryl as well as carbon-centred radicals needs to be considered;[3,5,6] Nozaki and co-workers have reported that anionic ligands and Lewis bases can stabilise boryl radicals, although calculations proposed the carbon-centred radical was the major resonance contributor.[5] Subsequently, they reported the reductive coupling of oxazoline-stabilised difluoroborane **5** in the absence of stirring (Scheme 2).[3] One electron reduction by KC_8 was proposed to form the boryl radical **6a** following loss of a fluoride and coupling of the carbon-centred radicals

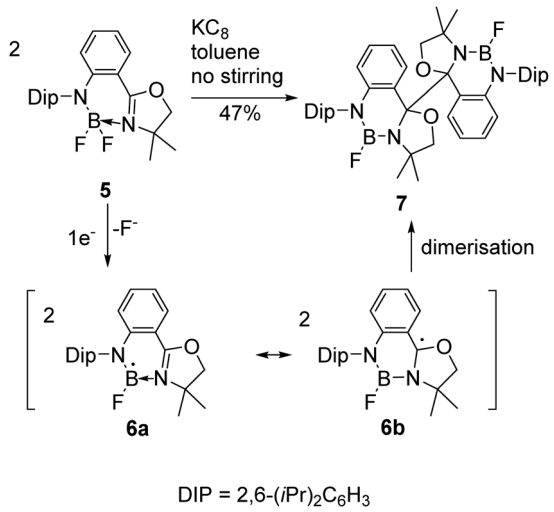

Scheme 2 Nozaki's reductive coupling of base-stabilised difluoroborane **5** where one electron reduction by KC_8 and loss of fluoride is proposed to form boryl radical **6a**. Dimerisation of the carbon-centred radical **6b** in the absence of stirring gives **7**.

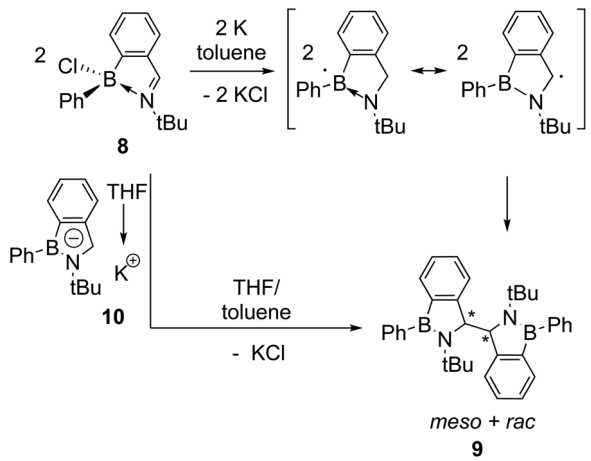

Scheme 3 Dostál's reductive coupling of iminochloroborane **8** forming dimer **9** as a mixture of *meso* and *rac* diastereomers. The two proposed mechanisms for dimer formation are depicted in analogy to those in Scheme 1.

6b under diffusion control led to dimer **7** formation in 47% yield.

Similarly, Dostál and co-workers reported the reductive coupling of iminochloroborane **8** with potassium produces a mixture of the *meso* and *rac* diastereomeric dimers **9** (Scheme 3).[6] The two diastereomers could be separated by fractional crystallisation and the *meso* isomer was observed to convert to the *rac* isomer quantitatively upon heating in toluene. Two similar mechanisms to the analogous reductive couplings of imines and carbonyl compounds were proposed, involving the coupling of two carbon-centred radicals following one electron reduction or the reaction of the BN-indenyl anion **10** (formed by 2 electron reduction) with iminochloroborane **8**.

Synthesis of amidoboronates

Reductive coupling of *N*-aryl iminoboronates

N-Aryl iminoboronates can be prepared exploiting dynamic covalent chemistry from three simple building blocks (Scheme 4): an aniline (blue), 2-formylphenyl boronic acid (red) and a diol (black).[54–56] Iminoboronates have been used in the self-assembly of macrocycles and cages,[55,57] determining the enantiomeric excess of amines and amino acids *via* fluorescent sensing,[58,59] self-healing polymers,[60,61] bioconjugation[62–66] and drug delivery applications.[67–69] These applications typically exploit the dynamic covalent nature of the imine and boronate bonds (see Dynamic Covalent Chemistry), however, the reactivity of the imine has been underexplored.

Given the structural similarity of iminoboronates to iminochloroborane **8** (Scheme 3), new BN-heterocycles could be potentially accessed as a mixture of diastereomeric $meso_5$† and rac_5† dimers *via* a reductive coupling of the imine. Furthermore, an advantage of iminoboronates is that a large family of substrates with different steric and electronic properties can be readily prepared by varying the building blocks during the iminoboronate self-assembly. Thus, we investigated the reductive coupling of *N*-aryl iminoboronates using reductants such as cobaltocene and decamethylcobaltocene, initially focusing on two series of iminoboronates (**1** and **2**) where the *para*-substituent of the aniline and the catechol were varied to investigate electronic effects (Scheme 5).[70,71]

The reductive couplings were initially performed in CD_3CN, monitoring the reaction progress by NMR spectroscopy where the loss of the imine signal was observed. In most reductive couplings two new sets of ^1H signals appeared including two methine signals between 5–6 ppm, attributed to the formation of a $meso_5$ and rac_5 diastereomeric mixture based on subsequent NMR analysis (see below, Solution characterisation). However, it was not possible to quantify the amount of the $meso_5$ and rac_5 diastereomers since one of the amidoboronate products typically crystallised from the reaction mixture of the reductive couplings (Table 1). Nevertheless, these crystals enabled the isolation and characterisation of single amidoboronate isomers both in the solid-state and in solution by redissolving the crystals in DMSO-d_6.

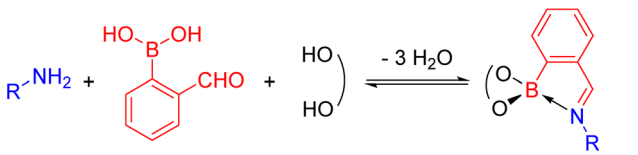

Scheme 4 Self-assembly of a *N*-aryl iminoboronate, the substrate for the reductive couplings, *via* dynamic covalent chemistry from an amine, 2-formylphenylboronic acid and a diol.

† In the naming of the isomers, the subscripts 5 and 6 refer to the heterocyclic ring size following dimerisation.

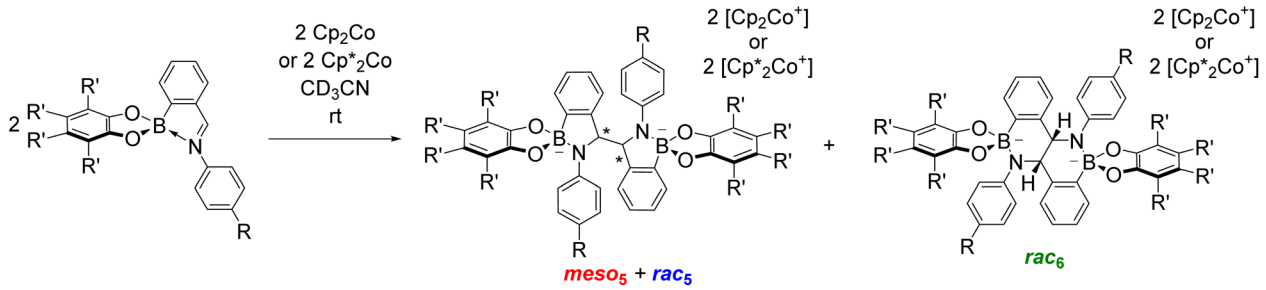

1a R = Cl, R' = H
1b R = F, R' = H
1c R = Me, R' = H
1d R = OMe, R' = H
1e R = NMe_2, R' = H
1f R = tBu, R' = H

2a R = Cl, R' = Cl
2b R = F, R' = Cl
2c R = Me, R' = Cl
2d R = OMe, R' = Cl
2e R = NMe_2, R' = Cl

3a R = Cl, R' = H
3b R = F, R' = H
3c R = Me, R' = H
3d R = OMe, R' = H
3e R = NMe_2, R' = H
3f R = tBu, R' = H

4a R = Cl, R' = Cl
4b R = F, R' = Cl
4c R = Me, R' = Cl
4d R = OMe, R' = Cl
4e R = NMe_2, R' = Cl

Scheme 5 The synthesis of up to three amidoboronate products (*meso*$_5$, *rac*$_5$ and *rac*$_6$) from the reductive coupling of *N*-aryl iminoboronates (pyrocatechol series: **1a–1e**; tetrachlorocatechol series **2a–2e**) using cobaltocene or decamethylcobaltocene.

Table 1 Summary of the isomers obtained *via* crystallisation from the reductive couplings in acetonitrile

***meso*$_5$**	***rac*$_5$**	***rac*$_6$**
[**3a**]$(Cp_2Co)_2$	[**3e**]$(Cp_2Co)_2$ [a]	[**3a**]$(Cp_2Co)_2$
[**3b**]$(Cp_2Co)_2$	[**4a**]$(Cp^*_2Co)_2$	[**3b**]$(Cp_2Co)_2$
	[**4c**]$(Cp_2Co)_2$	[**3c**]$(Cp_2Co)_2$
	[**4c**]$(Cp^*_2Co)_2$	[**3d**]$(Cp_2Co)_2$
	[**4d**]$(Cp_2Co)_2$	[**3f**]$(Cp_2Co)_2$
	[**4d**]$(Cp^*_2Co)_2$ [a]	
	[**4e**]$(Cp_2Co)_2$	
	[**4e**]$(Cp^*_2Co)_2$	

[a] The isomer was characterised in the solution state only by NMR spectroscopy.

Solid-state characterisation

X-ray crystal structures of [***meso*$_5$-3a**]$(Cp_2Co)_2$ and [***meso*$_5$-3b**]$(Cp_2Co)_2$ were obtained showing the *meso* isomer in two different conformations, *anti* and *gauche* (Fig. 2a and b). X-ray analysis of crystals obtained from the tetrachlorocatechol series (R′ = Cl) revealed the *rac*$_5$ isomer crystallised as the cobaltocenium and/or decamethylcobaltocenium salts (Fig. 2c).[70,71] For **4c**, crystal structures of three polymorphs of the cobaltocenium salt were obtained in addition to one crystal structure of the decamethylcobaltocenium salt. The X-ray crystal structures of the *meso*$_5$ and *rac*$_5$ isomers confirmed dimerisation *via* C–C bond formation between the two five-membered rings and Fig. 2 highlights the different stereochemistry around the new C–C bond for the two diastereomers using Newman projections.

Unexpectedly, X-ray analysis of crystals obtained from analogous reductive couplings of **1a** and **1b** on separate occasions were not *meso*$_5$ or *rac*$_5$ structures but an isomeric and previously unknown B–N heterocyclic scaffold consisting of two fused six-membered rather than five-membered rings (Fig. 2d). Thus, these amidoboronates were named the *rac*$_6$† product and similar X-ray crystal structures were obtained of [***rac*$_6$-3c,d,f**]$(Cp_2Co)_2$ in the pyrocatechol series (R′ = H). Since significant quantities of the *rac*$_6$ product were not observed in the reaction mixtures in CD_3CN, further studies in DMSO-d_6 (see below, Solution characterisation) probed whether it forms in the solid state only or also in solution.

Unlike the tetrachlorocatechol series where crystals were obtained of the *rac*$_5$ isomer only, crystals of all three isomers were obtained from the pyrocatechol series (Table 1). Amidoboronates **3a–b** containing electron-withdrawing Cl and F aniline substituents crystallised as either the *meso*$_5$ or *rac*$_6$ isomer (depending on the reaction conditions) and **3a–d,f** crystallised as the *rac*$_6$ isomer. Although crystals were also obtained from the reductive coupling of **3e**, they were not suitable for X-ray analysis. However, subsequent solution studies revealed the *rac*$_5$ isomer crystallised.

The number of crystal structures of the amidoboronate isomers as well as several iminoboronate starting materials has enabled comparison of different structural parameters (Table 2). Firstly, the formation of covalent B–N bonds in the amidoboronate products is confirmed by the shortening of the B–N bond (1.50–1.55 Å) compared to the dative B–N bond (1.66–1.68 Å) in the iminoboronate. In addition, the two counterions (Cp_2Co^+ or $Cp^*_2Co^+$) per dimer indicated the formation of two anionic tetrahedral boron centres. A slight lengthening of the B–O bonds was also observed in the amidoboronates compared to the iminoboronates.

The X-ray structures also revealed the conformation and bond length of the newly formed C–C bond (Table 2). The thermodynamic stability of the *gauche* and *anti* conformations has been reported for dimers formed from carbon-centred radicals.[72,73] Indeed, the *gauche* conformation (59–70°) was observed in all crystal structures except for ***meso*$_5$-3a** where the *anti* conformation (179°) was observed, likely due to different crystallisation conditions. Furthermore, the C–C bond lengths for all isomers (1.53–1.57 Å) were consistent with a sp^3-hybridised C–C bond, suggesting bond lengthening due to a contri-

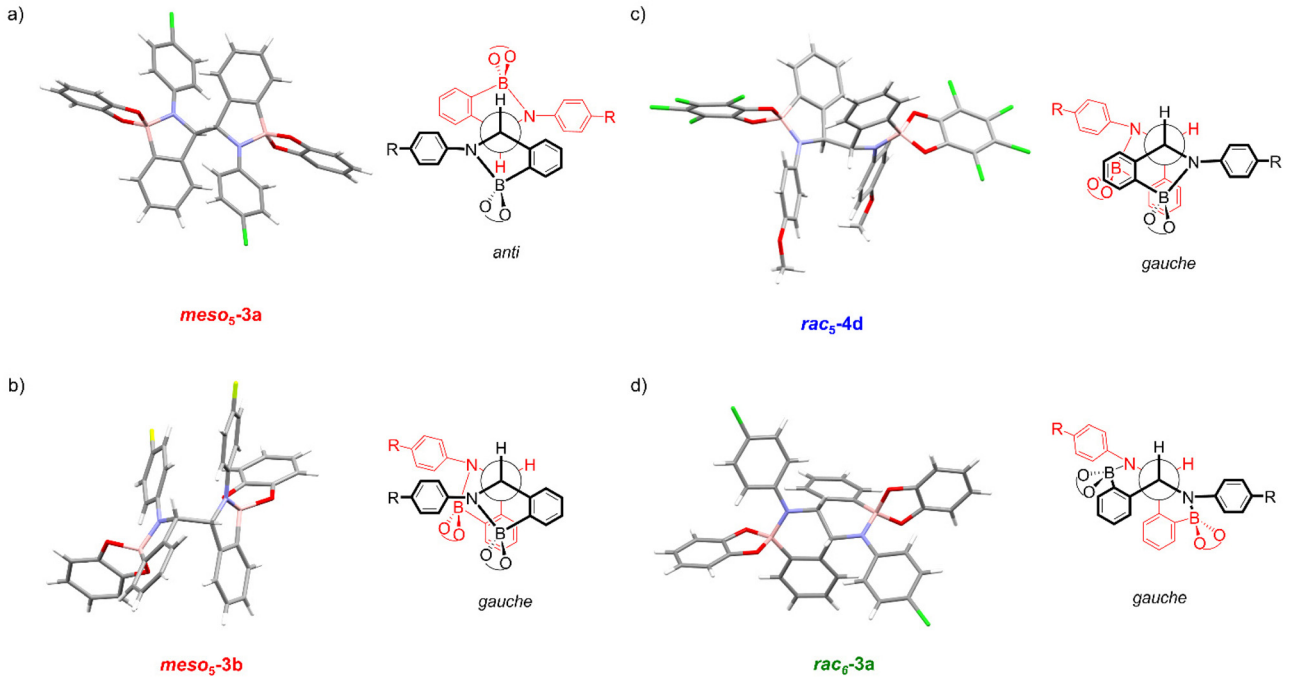

Fig. 2 X-ray crystal structures and Newman projections of: (a) [***meso*$_5$-3a**](Cp$_2$Co)$_2$; (b) [***meso*$_5$-3b**](Cp$_2$Co)$_2$; (c) [***rac*$_5$-4d**](Cp$_2$Co)$_2$; (d) [***rac*$_6$-3a**](Cp$_2$Co)$_2$. For clarity, the X-ray structures do not depict the Cp_2Co^+ countercations and solvent molecules. The Newman projections do not depict the R and catechol substituents and the two halves of the dimer are shown in red and black, particularly to show the change in connectivity in the *rac*$_6$ isomer. Adapted with permission from ref. 71.

Table 2 Overview of the HC–CH torsion angles and bond lengths for the C–C, B–N and B–O bonds from the X-ray crystal structures of iminoboronates and amidoboronates

	HC–CH (°)	C–C (Å)	B–N (Å)	B–O (Å)	Ref.
1a	—	—	1.68	1.47–1.46	71
1d	—	—	1.68	1.46–1.47	71
1e	—	—	1.68	1.46–1.48	71
2d	—	—	1.66	1.48–1.49	71
***meso*$_5$-3a**	179	1.56	1.55	1.51–1.52	71
***rac*$_6$-3a**	65	1.54	1.54	1.52–1.54	71
***meso*$_5$-3b**	64	1.58	1.53	1.52–1.53	70
***rac*$_6$-3b**	65	1.54	1.53	1.52–1.54	70
***rac*$_6$-3c**	65	1.53	1.53	1.53–1.54	70
***rac*$_6$-3d**	64	1.55	1.52	1.51–1.54	70
***rac*$_6$-3f**	64	1.54	1.54	1.51–1.54	70
***rac*$_5$-4a**	61	1.56	1.52	1.54	71
***rac*$_5$-4c**	60–70[a]	1.54–1.57[a]	1.50–1.51[a]	1.52–1.56[a]	70
***rac*$_5$-4d**	68	1.55	1.51	1.53–1.55	71
***rac*$_5$-4e**	59–66[b]	1.55–1.56[b]	1.50–1.51[b]	1.53–1.56[b]	71

[a] Based on the X-ray crystal structures of three polymorphs of the cobaltocenium salt and one crystal structure of the decamethylcobaltocenium salt. [b] Based on the X-ray crystal structures of the cobaltocenium and decamethylcobaltocenium salts.

bution from the radical form is minimal at the temperature of the measurements (100 K or 180 K).

Solution characterisation

As revealed by X-ray analysis, up to three isomeric amidoboronates crystallised from the reductive couplings in CD_3CN. The solution structure of the *meso*$_5$, *rac*$_5$ and *rac*$_6$ isomers was probed by redissolving the isolated crystals in DMSO-d_6. Regardless of the substitution of the amidoboronates, characteristic signals were observed for each product: a methine signal around 5.4 ppm for the *meso*$_5$ diastereomer; a methine signal around 5.2 ppm and doublet around 7.7 ppm for the *rac*$_5$ diastereomer; a methine signal around 4.9 ppm and two doublets around 6.9 and 6.8 ppm for the *rac*$_6$ isomer. Similar shifts were observed for the amidoboronate products in both DMSO-d_6 and CD_3CN, enabling identification of the isomeric mixtures in the corresponding reductive couplings in CD_3CN.

The existence of the *rac*$_6$ product in solution was investigated in time-course NMR experiments (Scheme 6).[70] For the reductive coupling of **1f** in CD_3CN where the *rac*$_6$ isomer crystallised from the reaction mixture, the *rac*$_5$ signals were observed to decrease over time and this enabled the characterisation of the remaining isomer in solution, ***meso*$_5$-3f**. In analogous reductive couplings with **1b** and **1d** in DMSO-d_6 where crystallisation was prevented, the *meso*$_5$ and *rac*$_5$ diastereomers initially formed and the *rac*$_5$ converted into the *rac*$_6$ isomer over time, as evidenced by the appearance of a third methine signal consistent with redissolved *rac*$_6$ crystals. Thus, the *rac*$_6$ isomer was proposed to form *via* breakage and rearrangement of the covalent B–N bonds in the *rac*$_5$ isomer. The following sections introduce dynamic covalent chemistry with a focus on examples relevant to the subsequent discussion of the dynamic covalent chemistry of amidoboronates, including the B–N bonds in more detail.

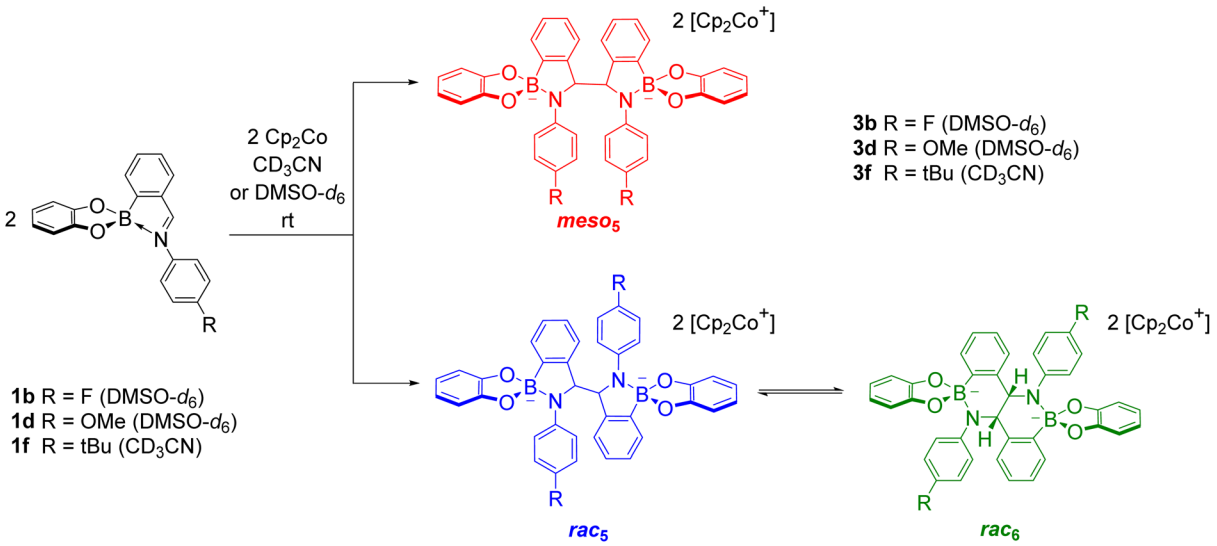

Scheme 6 Time-course NMR experiments in CD_3CN (for **1f**) or DMSO-d_6 (for **1b** and **1d**) suggested the initial formation of the *meso*$_5$ and *rac*$_5$ diastereomers followed by interconversion of the *rac*$_5$ isomer into the *rac*$_6$ *via* rearrangement of the dynamic covalent B–N bonds.

Dynamic covalent chemistry

Dynamic covalent chemistry[15–19] is a diverse research field encompassing a variety of reversible covalent bonds from C=N[22,24–28] to B–O[19,22,32–34] bonds. The combination of several dynamic covalent bonds offers the potential for addressing the different functional groups orthogonally, thus increasing the complexity of the system.

N-Aryl iminoboronates (the substrates for the synthesis of amidoboronates) contain two types of dynamic covalent bonds, an imine and boronate ester, leading to synergistic effects during their self-assembly from an aniline, diol and 2-formylphenyl boronic acid (Scheme 4). Nitschke and co-workers reported the amine and diol subcomponents influence the stability and yield of the resulting iminoboronate;[55] synergistic stabilisation of the imine and boronate ester was proposed from the combination of an electron-rich aniline and catecholate due to greater resonance delocalisation over the catecholate, resulting in a B–N dative bond in aprotic solvents. In contrast, incomplete iminoboronate formation was observed with an electron-rich aniline and an electron-rich alkoxide, attributed to increased electron density around the boron centre leading to destabilisation and the absence of a B–N dative bond.

In addition, both the aniline and diol subcomponents can be orthogonally exchanged when a thermodynamically more stable iminoboronate results from exchange.[55] More electron-rich amines (*e.g.* an alkylamine) replaced electron-poor ones (*e.g.* an aniline) driven by the formation of a more electron-rich imine stabilising the boron centre (Scheme 7a). Furthermore, aliphatic diols were displaced by pyrocatechol due to better delocalisation of the oxygens' partial negative charge over the aromatic catechol (Scheme 7b).

While combinations of two types of dynamic covalent bonds can be orthogonally exchanged (*e.g.* imines and boronate esters as in Scheme 7),[74] extension to three dynamic covalent bonds introduces additional orthogonality issues. Matile and co-workers investigated the orthogonality of hydrazone (red, Scheme 8a), boronate ester (green) and disulfide (blue) bonds in multicomponent self-assembly **11** as well as model systems like **12** (Scheme 8b) and increasing the stability of the boronate ester was necessary for orthogonality under the acidic hydrazone exchange conditions.[22] This was achieved using the boronate esters of benzoboroxoles where the anionic

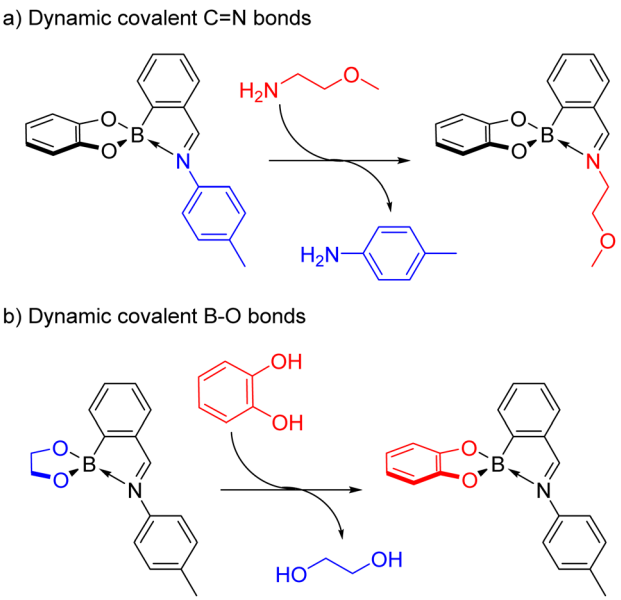

Scheme 7 Orthogonal dynamic covalent bonds reported by Nitschke and co-workers in *N*-aryl iminoboronates involving: (a) imine exchange of an aniline subcomponent for a more electron-rich alkylamine; (b) boronate ester exchange of an aliphatic diol for pyrocatechol.

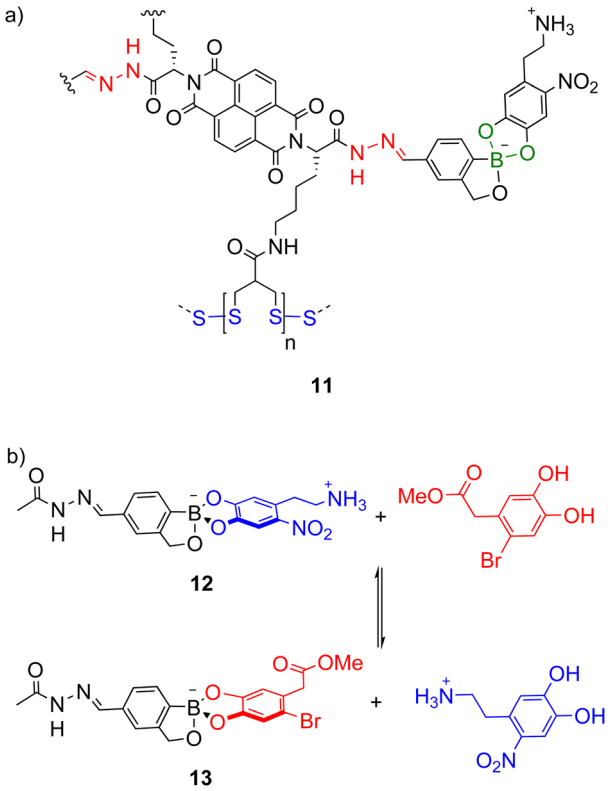

Scheme 8 Matile's (a) multicomponent assembly **11** with three types of orthogonal dynamic covalent bonds: hydrazone (red), boronate ester (green) and disulfide (blue); (b) model system **12** for investigating the stability of the boronate ester under the conditions for hydrazone, boronate ester and disulfide exchange.

tetrahedral boron centre is proposed to be less electrophilic and intramolecularly stabilised. In model system **12**, the boronate ester was stable under the acidic hydrazone exchange conditions and basic disulfide exchange conditions but under the boronate ester exchange conditions (DMSO-d_6, 10% D_2O, 2% Hünig's base), equilibrium was reached in under 3 min giving a 1 : 1.1 mixture of **12** and **13** (Scheme 8b).

There could be parallels between the dynamic covalent chemistry of amidoboronates and the examples shown in Schemes 7 and 8. However, there are some differences since reductive coupling of the imine bond removes the possibility of imine exchange in amidoboronates. Nevertheless, there is also the potential to access new types of dynamic covalent bonds in amidoboronates, for example dynamic covalent C–C bonds through the involvement of radicals during the reductive coupling based on literature examples.

While C–C bond formation from the dimerisation and dissociation of organic radicals has been long known (Scheme 9),[75–78] its application in dynamic covalent chemistry has only recently emerged.[18] To ensure the necessary reversibility, several conditions need to be fulfilled: a relatively low bond dissociation enthalpy to establish the radical/dimer equilibrium under mild conditions; sufficient thermodynamic stabilisation of the radical (*e.g.* by improving spin delocalisation through expansion of the π system and/or substitution[18,79,80]) so that the equilibrium shifts towards the radical; suppression of side-reactions given the reactivity of radicals.[18] A number of carbon-based radicals including dicyanomethyl,[72,73,79,81–83] fluorenyl,[80] lactone[80,84] and 4-substituted triphenylmethyl[85] derivatives have already been shown to undergo reversible C–C bond formation (Scheme 9), enabling the self-assembly of macrocycles[72,73,79,82,86,87] and the development of stimuli-responsive materials.[81,84]

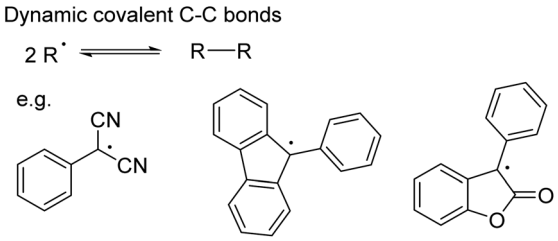

Scheme 9 Dynamic covalent C–C bond formation involving radicals, such as dicyanomethyl, fluorenyl and lactone derivatives.

Dynamic covalent chemistry of amidoboronates

Amidoboronates are thus interesting candidates for use in dynamic covalent chemistry applications given the initial implication of dynamic covalent B–N bonds in the rac_5/rac_6 rearrangement and the potential for dynamic covalent C–C and B–O bonds. The dynamic covalent chemistry of the amidoboronates was explored and of particular interest was the discovery of new chemistry, for example compared to iminoboronates and other reductively coupled dimers.

C–C bonds

The reversibility of C–C bond formation was investigated in a series of experiments to gain insight into the reductive coupling mechanism. Based on the analogous reductive coupling of iminochloroborane **8** reported by Dostál and co-workers (see Synthesis of B-N heterocyclic dimers),[6] radicals are proposed to be involved. Firstly, isolated crystals of the $meso_5$, rac_5 and rac_6 isomers were redissolved in DMSO-d_6 to probe the existence of a radical/dimer equilibrium. However, there has been thus far no evidence of a conversion between the $meso_5$ and *rac* isomers at room temperature *via* reversible C–C bond formation in the redissolved crystals. Furthermore, decomposition was observed upon heating solutions of the redissolved crystals of ***meso*$_5$-3b** and ***rac*$_6$-3c** at elevated temperatures (90 °C or above).[70] This contrasts the finding by Dostál and co-workers that ***meso*-9** can be converted to ***rac*-9** upon heating in toluene (Scheme 3).[6]

However, the addition of the tritylium cation to an isomeric mixture of **3c** or **4c** led to quantitative regeneration of the corresponding iminoboronates **1c** or **2c** at room temperature within 10 minutes (Scheme 10). The tritylium cation acts as an

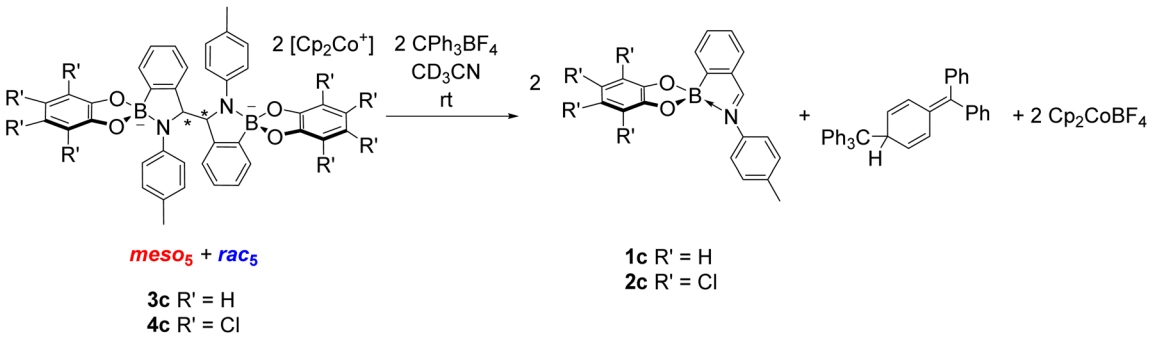

Scheme 10 Addition of the tritylium cation to an isomeric mixture of **3c** or **4c** regenerates the corresponding iminoboronate (**1c** or **2c**) as well as the trityl dimer and Cp_2CoBF_4. For clarity, only the *meso*$_5$ and *rac*$_5$ isomers are depicted as they were the major species observed in the reaction mixture in CD_3CN.

electron abstractor leading to oxidative decoupling of the dimers as well as Cp_2CoBF_4 and the formation of the trityl dimer from subsequent radical coupling. This ability to break the newly formed C–C bond in the dimer has not been reported in the related reductive couplings of imine and carbonyl compounds (see Synthesis of 1,2-diamines and 1,2-diols).

In another experiment, the TEMPO radical was added to an isomeric mixture of **4c** and upon heating at 70 °C in CD_3CN for 3 days, an additional species appeared in the ^{1}H NMR spectrum (Fig. 3a).[70] X-ray analysis of crystals obtained from the reaction revealed the formation of **14** where TEMPO rather than the imine is coordinated to the anionic tetrahedral boron centre (Fig. 3b). The formation of an imine was also consistent with the observation of a singlet above 9 ppm for the new species in the NMR spectrum. The formation of **14** was proposed *via* electron abstraction from the nitrogen lone pair by TEMPO giving a nitrogen-based radical cation, homolytic cleavage of the C–C bond generating an imine and finally, nucleophilic attack of TEMPO$^-$ on the boron centre. This contrasts the formation of radicals *via* homolytic substitution of trigonal catecholborane derivatives by TEMPO.[88–90]

These experiments demonstrated that the new C–C bond can be broken upon addition of an electron abstractor (CPh_3^+) or a radical (TEMPO). The existence of a radical/dimer equilibrium will be probed in future experiments to investigate whether the reductive coupling can be implemented for the formation of dynamic covalent C–C bonds like in Scheme 9.

B–N bonds

The reductive coupling converts the B–N dative bond observed in iminoboronates **1a–1f** and **2a–2e** to covalent B–N bonds with anionic tetrahedrally coordinated boron centres. Unexpectedly, these covalent B–N bonds were found to be dynamic as the rearrangement of the *rac*$_5$ into the *rac*$_6$ isomer was observed over time in time-course NMR experiments (see Solution characterisation). In contrast, redissolved crystals of ***meso*$_5$-3a–b** did not interconvert into either of the *rac* isomers and there has been no evidence thus far of the formation of a *meso*$_6$ product.

The *rac*$_5$/*rac*$_6$ rearrangement was investigated in more detail by redissolving isolated crystals in DMSO-d_6 (Scheme 11). Initial investigations suggested increased electron density facilitates cleavage of the B–N bond since the rate of interconversion of **3b,c–f** was qualitatively fastest with **3d** containing the most electron-donating aniline substituents in the series.[70]

Further investigations focused on the amount of the *rac*$_5$ and *rac*$_6$ isomers following equilibration as a function of the *para*-substituent on the aniline and the catechol (Fig. 4).[71] For the pyrocatechol series, ***rac*$_6$-3a,c–d** and ***rac*$_5$-3e** crystallised from the reductive couplings. While ***rac*$_6$-3a** did not interconvert to the *rac*$_5$ isomer, the amount of the *rac*$_5$ isomer for the other derivatives increased with more electron-donating substituents (Scheme 11a, Fig. 4a). A 1 : 1 *rac*$_5$/*rac*$_6$ mixture was obtained for **3e** with the most electron-rich NMe_2 substituent.

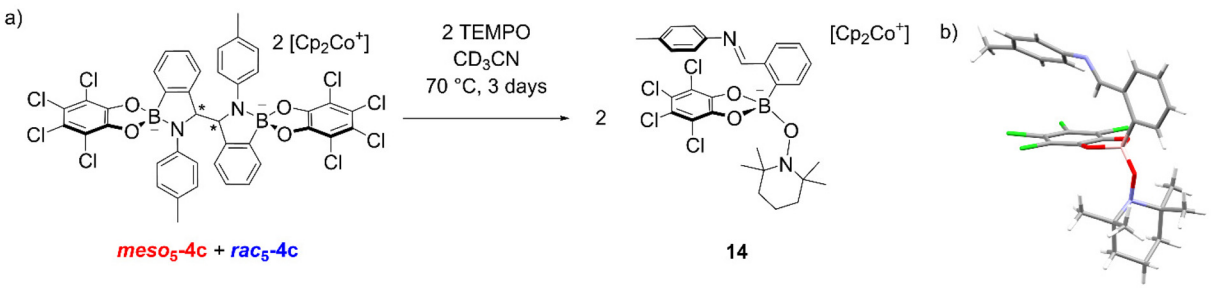

Fig. 3 (a) Formation of **14** from the reaction of a **4c** isomeric mixture with the TEMPO radical. For clarity, only the major amidoboronate species in solution are depicted; (b) X-ray crystal structure of **14** with Cp_2Co^+ countercation removed for clarity.

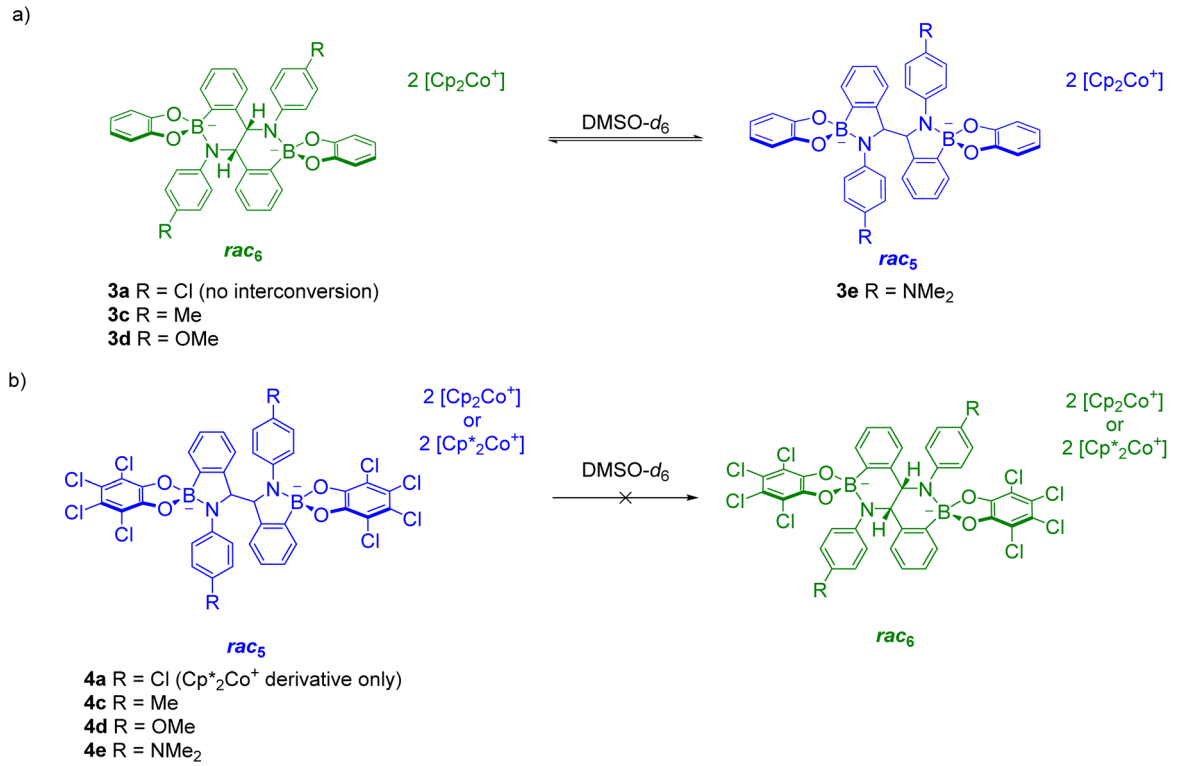

Scheme 11 rac_5/rac_6 interconversion upon redissolving crystals of (a) rac_6-**3a,c–d** and rac_5-**3e**; (b) rac_5-**4a,c–e**. Adapted with permission from ref. 71.

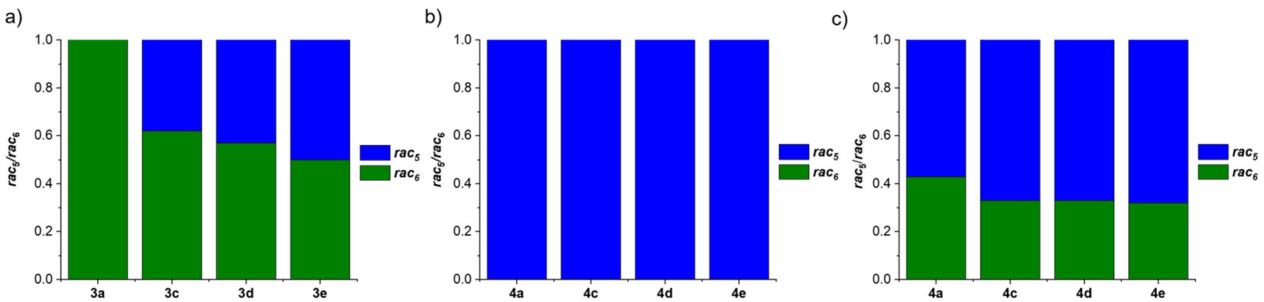

Fig. 4 Comparison of the rac_5/rac_6 isomeric ratios following: (a) equilibration of redissolved crystals of **3a,c–e** from the pyrocatechol series; (b) equilibration of redissolved crystals of **4a,c–e** from the tetrachlorocatechol series; (c) catechol exchange of pyrocatechol for tetrachlorocatechol in equilibrated rac_5/rac_6 mixtures from (a). Reprinted with permission from ref. 71.

In contrast, redissolved rac_5 crystals as either the cobaltocenium or decamethylcobaltocenium salt from the tetrachlorocatechol series (**4a,c–e**) were not observed to interconvert to the rac_6 isomer (Scheme 11b, Fig. 4b).

Conformational analysis of the rac_5 and rac_6 isomers may provide an explanation for the rac_5/rac_6 rearrangement (Fig. 5). Of the three most likely conformations (two *gauche* and one *anti*), only the *gauche* conformation (black box) where the anilines are *anti* to one another has been observed in the X-ray crystal structures (Fig. 2c). A similar *gauche* conformation (black box, Fig. 5) was also observed in the X-ray crystal structures of the rac_6 isomer (Fig. 2d), suggesting that the rac_5/rac_6 rearrangement occurs *via* breakage of the B–N bonds and rotation of the phenylboronate ester groups so that the five-membered rings are converted to a fused six-membered ring scaffold. Fig. 5 represents the two halves of the rac_5 dimer in red and black to highlight the change of the connectivity in the rac_6 isomer where the red nitrogen forms a covalent bond to the boron centre in black and *vice versa*.

Based on the observed interconversions (Scheme 11), electronic effects were proposed to control the rac_5/rac_6 rearrangement; an electron-withdrawing Cl aniline substituent (**3a**) or catechol such as tetrachlorocatechol (**4a,c–e**) resulted in no interconversion of the rac_6 and rac_5 isomers, respectively, attributed to strengthening of the B–N bond from the reduced electron density. However, increasing the electron density in

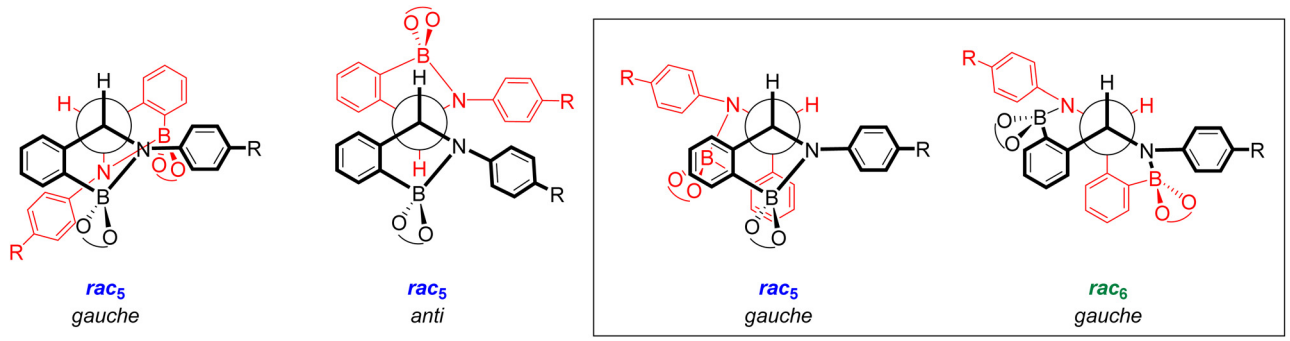

Fig. 5 Conformational analysis of the rac_5 isomer showing the three possible conformations around the new C–C bond, two *gauche* and one *anti*. Black box: the *gauche* conformations of the rac_5 and rac_6 isomers observed in X-ray crystal structures. The red and black represent the two halves of the dimer to highlight the change in connectivity upon the rac_5/rac_6 rearrangement.

the B–N bond through more electron-donating aniline substituents is proposed to weaken the B–N bond, resulting in increased rac_5/rac_6 interconversion.

B–O bonds

The diol subcomponents within boronate ester bonds are known to undergo exchange *via* dynamic covalent B–O bonds.[19,22,55,74] However, in most cases the boron centre has a vacant p orbital (*e.g.* in iminoboronates in the absence of a BN dative bond, Scheme 7b), whereas in amidoboronates this is filled since the boron is anionic and tetrahedrally coordinated. Nevertheless, Matile and co-workers reported catechol exchange with boronate esters of benzoboroxoles containing anionic tetrahedral boron centres (Scheme 8b).[22] Therefore, the dynamic covalent nature of the B–O bonds of amidoboronates was explored in catechol exchange experiments.[71]

Addition of tetrachlorocatechol to equilibrated mixtures of ***rac*-$_5$/*rac*$_6$-3a,c–e** in DMSO-d_6 led to complete catechol exchange and the formation of ***rac*$_5$/*rac*$_6$-4a,c–e** (Scheme 12). The rac_5/rac_6 ratio was changed from a preference for the rac_6 isomer prior to catechol exchange (Fig. 4b) to a preference for the rac_5 isomer (Fig. 4c). The presence of the rac_6 isomer following catechol exchange is attributed to the catechol exchange pathway allowing the direct conversion of ***rac*$_6$-3** to ***rac*$_6$-4** rather than *via* the rac_5/rac_6 interconversion since redissolved ***rac*$_5$-4** crystals did not interconvert to the rac_6 isomer.

While catechol exchange of pyrocatechol for the more electron-deficient tetrachlorocatechol was observed, addition of excess pyrocatechol to ***rac*$_5$-4d** showed no catechol exchange. It

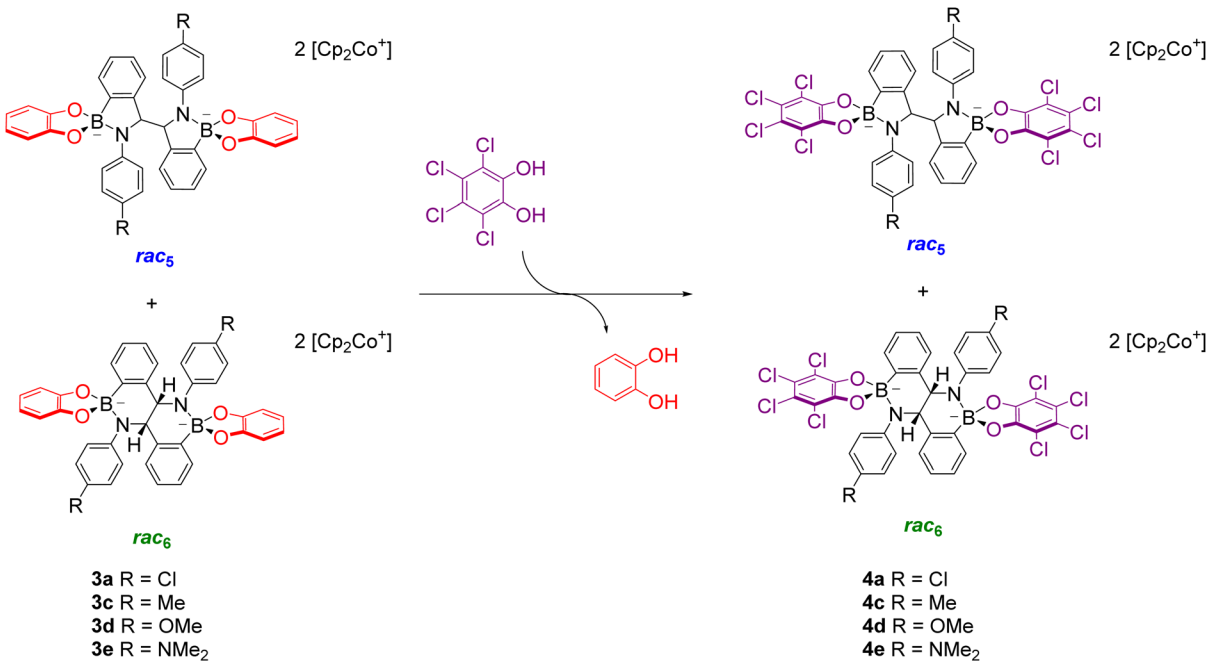

3a R = Cl
3c R = Me
3d R = OMe
3e R = NMe_2

4a R = Cl
4c R = Me
4d R = OMe
4e R = NMe_2

Scheme 12 Boronate ester exchange of pyrocatechol for tetrachlorocatechol *via* dynamic covalent B–O bonds converts an equilibrated mixture of ***rac*$_5$-3** and ***rac*$_6$-3** to ***rac*$_5$-4** and ***rac*$_6$-4**. Adapted with permission from ref. 71.

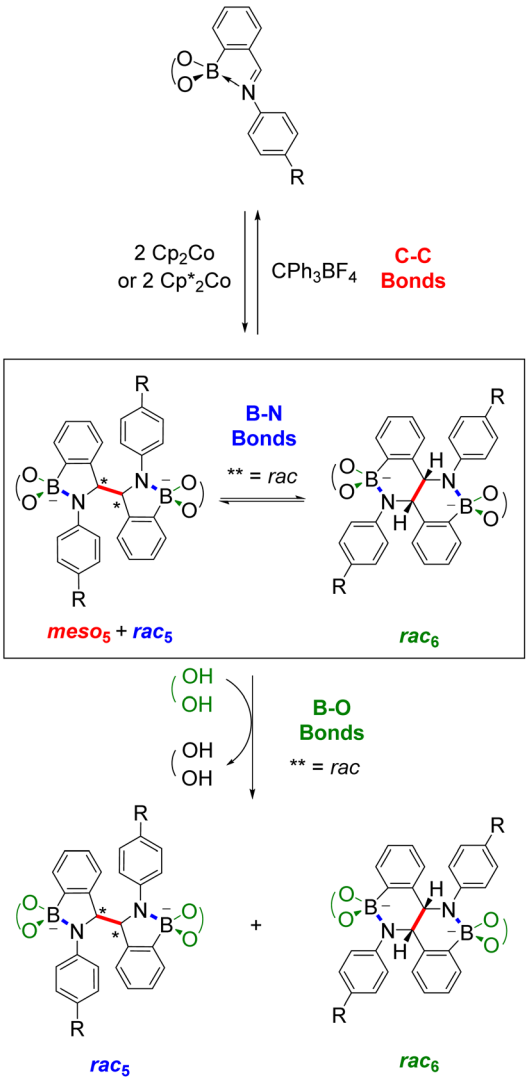

Scheme 13 Overview of the synthesis and dynamic covalent chemistry of amidoboronates showing the three types of dynamic covalent bonds (C–C in red, B–N in blue and B–O in green). For clarity, the R groups, catechols and countercations are not depicted.

was proposed that the tetrachlorocatechol analogues are thermodynamically more stable due to better negative charge delocalisation with tetrachlorocatechol *vs.* pyrocatechol and this is the driving force for catechol exchange.

Conclusions and outlook

While the number of synthetic methods for BN-heterocycles are limited compared to their carbon analogues, this is an active field with an increasing number of reports particularly given the growing importance of BN-heterocycles in catalysis and materials chemistry applications. On the other hand, dynamic covalent chemistry is an established field but new applications and types of dynamic covalent bonds (*e.g.* based on radicals[18]) are emerging.

Amidoboronates bring together BN-heterocyclic synthesis and dynamic covalent chemistry and new research directions have been made possible through this intersection of these two seemingly disconnected research fields. Amidoboronates are a new class of BN-containing heterocycles that can be prepared from *N*-aryl iminoboronate substrates *via* a reductive coupling (Scheme 13). Their synthesis opens up new chemical space since up to three isomers can be prepared from a single substrate, which itself can be modularly self-assembled from three building blocks using dynamic covalent chemistry. Thus, a large family of new BN-heterocycles was synthesised with reduced effort.

In addition, initial studies have revealed the interesting and unusual dynamic covalent chemistry of amidoboronates involving C–C, B–N and B–O bonds. Unlike the analogous reductive couplings of carbonyls and imines, C–C bond formation is reversible for amidoboronates since oxidative decoupling of the dimer through the addition of the tritylium cation regenerates the iminoboronate. An unprecedented rearrangement between the rac_5 and rac_6 isomers *via* dynamic covalent B–N bonds has also been observed where the aniline *para*-substituent and the catechol tune the isomeric ratio at equilibrium. Furthermore, boronate ester exchange can be exploited as another tool to control this ratio.

Further exploration of this chemical space will offer new opportunities for applications of this chemistry. Future efforts will focus on exploring the mechanism of the reductive coupling, particularly to control the diastereoselectivity and therefore, selectively synthesise a particular isomer. The three types of dynamic covalent bonds also offer an exciting opportunity for exploring the orthogonality of transformations and the design of more complex stimuli-responsive systems.

Conflicts of interest

There are no conflicts to declare.

Acknowledgements

I would like to thank everyone who has contributed to this project and Patrick Harders for providing feedback on this manuscript. The Deutsche Forschungsgemeinschaft (DFG, project number 447862786) is gratefully acknowledged for financial support.

References

1 M. J. S. Dewar, V. P. Kubba and R. Pettit, *J. Chem. Soc.*, 1958, 3073–3076.
2 A. J. Ashe and X. Fang, *Org. Lett.*, 2000, **2**, 2089–2091.
3 M. Yamashita, Y. Aramaki and K. Nozaki, *New J. Chem.*, 2010, **34**, 1774–1782.

4 P. G. Campbell, A. J. V. Marwitz and S.-Y. Liu, *Angew. Chem., Int. Ed.*, 2012, **51**, 6074–6092.
5 Y. Aramaki, H. Omiya, M. Yamashita, K. Nakabayashi, S.-i. Ohkoshi and K. Nozaki, *J. Am. Chem. Soc.*, 2012, **134**, 19989–19992.
6 M. Hejda, R. Jambor, A. Růžička, A. Lyčka and L. Dostál, *Dalton Trans.*, 2014, **43**, 9012–9015.
7 X.-Y. Wang, J.-Y. Wang and J. Pei, *Chem. – Eur. J.*, 2015, **21**, 3528–3539.
8 M. M. Morgan and W. E. Piers, *Dalton Trans.*, 2016, **45**, 5920–5924.
9 Z. X. Giustra and S.-Y. Liu, *J. Am. Chem. Soc.*, 2018, **140**, 1184–1194.
10 K. Matsui, S. Oda, K. Yoshiura, K. Nakajima, N. Yasuda and T. Hatakeyama, *J. Am. Chem. Soc.*, 2018, **140**, 1195–1198.
11 C. R. McConnell and S.-Y. Liu, *Chem. Soc. Rev.*, 2019, **48**, 3436–3453.
12 H. Noda, Y. Asada, M. Shibasaki and N. Kumagai, *J. Am. Chem. Soc.*, 2019, **141**, 1546–1554.
13 C.-W. Ju, B. Li, L. Li, W. Yan, C. Cui, X. Ma and D. Zhao, *J. Am. Chem. Soc.*, 2021, **143**, 5903–5916.
14 F. Lindl, A. Lamprecht, M. Arrowsmith, E. Khitro, A. Rempel, M. Dietz, T. Wellnitz, G. Bélanger-Chabot, A. Stoy, V. Paprocki, D. Prieschl, C. Lenczyk, J. Ramler, C. Lichtenberg and H. Braunschweig, *Chem. – Eur. J.*, 2023, **29**, e202203345.
15 S. J. Rowan, S. J. Cantrill, G. R. L. Cousins, J. K. M. Sanders and J. F. Stoddart, *Angew. Chem., Int. Ed.*, 2002, **41**, 898–952.
16 S. P. Black, J. K. M. Sanders and A. R. Stefankiewicz, *Chem. Soc. Rev.*, 2014, **43**, 1861–1872.
17 R.-C. Brachvogel and M. von Delius, *Eur. J. Org. Chem.*, 2016, 3662–3670.
18 D. Sakamaki, S. Ghosh and S. Seki, *Mater. Chem. Front.*, 2019, **3**, 2270–2282.
19 S. Chatterjee, E. V. Anslyn and A. Bandyopadhyay, *Chem. Sci.*, 2021, **12**, 1585–1599.
20 C. G. Pappas, P. K. Mandal, B. Liu, B. Kauffmann, X. Miao, D. Komáromy, W. Hoffmann, C. Manz, R. Chang, K. Liu, K. Pagel, I. Huc and S. Otto, *Nat. Chem.*, 2020, **12**, 1180–1186.
21 N.-M. Phan, E. G. Percástegui and D. W. Johnson, *ChemPlusChem*, 2020, **85**, 1270–1282.
22 S. Lascano, K.-D. Zhang, R. Wehlauch, K. Gademann, N. Sakai and S. Matile, *Chem. Sci.*, 2016, 7, 4720–4724.
23 Y. Jin, Q. Wang, P. Taynton and W. Zhang, *Acc. Chem. Res.*, 2014, **47**, 1575–1586.
24 C. Liang, S. Kulchat, S. Jiang and J.-M. Lehn, *Chem. Sci.*, 2017, **8**, 6822–6828.
25 A.-E. Dascalu, L. Halgreen, A. Torres-Huerta and H. Valkenier, *Chem. Commun.*, 2022, **58**, 11103–11106.
26 B. P. Benke, T. Kirschbaum, J. Graf, J. H. Gross and M. Mastalerz, *Nat. Chem.*, 2023, **15**, 413–423.
27 Y. Wu, C. Zhang, S. Fang, D. Zhu, Y. Chen, C. Ge, H. Tang and H. Li, *Angew. Chem., Int. Ed.*, 2022, **61**, e202209078.
28 K. Caprice, D. Pál, C. Besnard, B. Galmés, A. Frontera and F. B. L. Cougnon, *J. Am. Chem. Soc.*, 2021, **143**, 11957–11962.
29 X. Wang, O. Shyshov, M. Hanževački, C. M. Jäger and M. von Delius, *J. Am. Chem. Soc.*, 2019, **141**, 8868–8876.
30 D. Hartmann and L. Greb, *Angew. Chem., Int. Ed.*, 2020, **59**, 22510–22513.
31 J. Roeser, D. Prill, M. J. Bojdys, P. Fayon, A. Trewin, A. N. Fitch, M. U. Schmidt and A. Thomas, *Nat. Chem.*, 2017, **9**, 977–982.
32 S. Ivanova, E. Köster, J. J. Holstein, N. Keller, G. H. Clever, T. Bein and F. Beuerle, *Angew. Chem., Int. Ed.*, 2021, **60**, 17455–17463.
33 N. Christinat, R. Scopelliti and K. Severin, *Angew. Chem., Int. Ed.*, 2008, **47**, 1848–1852.
34 N. Iwasawa and H. Takahagi, *J. Am. Chem. Soc.*, 2007, **129**, 7754–7755.
35 J. J. Eisch, D. D. Kaska and C. J. Peterson, *J. Org. Chem.*, 1966, **31**, 453–456.
36 J. G. Smith and C. D. Veach, *Can. J. Chem.*, 1966, **44**, 2497–2502.
37 J. G. Smith and I. Ho, *J. Org. Chem.*, 1972, **37**, 653–656.
38 E. J. Enholm, D. C. Forbes and D. P. Holub, *Synth. Commun.*, 1990, **20**, 981–987.
39 R. D. Rieke and S.-H. Kim, *J. Org. Chem.*, 1998, **63**, 5235–5239.
40 M. Shimizu, I. Suzuki and H. Makino, *Synlett*, 2003, 1635–1638.
41 R. J. Baker, C. Jones, M. Kloth and D. P. Mills, *New J. Chem.*, 2004, **28**, 207–213.
42 M. Nakajima, E. Fava, S. Loescher, Z. Jiang and M. Rueping, *Angew. Chem., Int. Ed.*, 2015, **54**, 8828–8832.
43 C.-M. Wang, P.-J. Xia, J.-A. Xiao, J. Li, H.-Y. Xiang, X.-Q. Chen and H. Yang, *J. Org. Chem.*, 2017, **82**, 3895–3900.
44 S. Kundu, L. Roy and M. S. Maji, *Org. Lett.*, 2022, **24**, 9001–9006.
45 Z. Qiu, H. D. M. Pham, J. Li, C.-C. Li, D. J. Castillo-Pazos, R. Z. Khaliullin and C.-J. Li, *Chem. Sci.*, 2019, **10**, 10937–10943.
46 A. Caron, É. Morin and S. K. Collins, *ACS Catal.*, 2019, **9**, 9458–9464.
47 M. Liu, L. Tan, R. T. Rashid, Y. Cen, S. Cheng, G. Botton, Z. Mi and C.-J. Li, *Chem. Sci.*, 2020, **11**, 7864–7870.
48 M. Yasui, K. Hanaya, T. Sugai and S. Higashibayashi, *RSC Adv.*, 2021, **11**, 24652–24655.
49 J. Jo, S. Kim, J.-H. Choi and W.-j. Chung, *Chem. Commun.*, 2021, **57**, 1360–1363.
50 Z.-W. Xi, L. Yang, D.-Y. Wang, C.-W. Feng, Y. Qin, Y.-M. Shen, C. Pu and X. Peng, *J. Org. Chem.*, 2021, **86**, 2474–2488.
51 Á. Péter, S. Agasti, O. Knowles, E. Pye and D. J. Procter, *Chem. Soc. Rev.*, 2021, **50**, 5349–5365.
52 F. Calogero, G. Magagnano, S. Potenti, F. Pasca, A. Fermi, A. Gualandi, P. Ceroni, G. Bergamini and P. G. Cozzi, *Chem. Sci.*, 2022, **13**, 5973–5981.
53 C. A. Rosengarten, K. Yuvaraj, L. F. Lim, N. Cox and C. Jones, *Chem. – Eur. J.*, 2023, **29**, e202300135.

54 H. E. Dunn, J. C. Catlin and H. R. Snyder, *J. Org. Chem.*, 1968, **33**, 4483–4486.
55 M. Hutin, G. Bernardinelli and J. R. Nitschke, *Chem. – Eur. J.*, 2008, **14**, 4585–4593.
56 R. R. Groleau, T. D. James and S. D. Bull, *Coord. Chem. Rev.*, 2021, **428**, 213599.
57 A. D. Herrera-España, H. Höpfl and H. Morales-Rojas, *Eur. J. Org. Chem.*, 2022, e202200383.
58 E. G. Shcherbakova, T. Minami, V. Brega, T. D. James and P. Anzenbacher, *Angew. Chem., Int. Ed.*, 2015, **54**, 7130–7133.
59 M. Pushina, S. Farshbaf, E. G. Shcherbakova and P. Anzenbacher, *Chem. Commun.*, 2019, **55**, 4495–4498.
60 S. Delpierre, B. Willocq, J. De Winter, P. Dubois, P. Gerbaux and J.-M. Raquez, *Chem. – Eur. J.*, 2017, **23**, 6730–6735.
61 S. Delpierre, B. Willocq, G. Manini, V. Lemaur, J. Goole, P. Gerbaux, J. Cornil, P. Dubois and J.-M. Raquez, *Chem. Mater.*, 2019, **31**, 3736–3744.
62 H. Faustino, M. J. S. A. Silva, L. F. Veiros, G. J. L. Bernardes and P. M. P. Gois, *Chem. Sci.*, 2016, **7**, 5052–5058.
63 M. K. Meadows, E. K. Roesner, V. M. Lynch, T. D. James and E. V. Anslyn, *Org. Lett.*, 2017, **19**, 3179–3182.
64 A. J. van der Zouwen, A. Jeucken, R. Steneker, K. F. Hohmann, J. Lohse, D. J. Slotboom and M. D. Witte, *Chem. – Eur. J.*, 2021, **27**, 3292–3296.
65 A. M. M. Rangaswamy, M. H. R. Beh, E. Soleimani, S. Sequeira, J. Cormier, K. N. Robertson and D. L. Jakeman, *J. Org. Chem.*, 2022, **87**, 13542–13555.
66 M. Zheng, F.-J. Chen, K. Li, R. M. Reja, F. Haeffner and J. Gao, *J. Am. Chem. Soc.*, 2022, **144**, 15885–15893.
67 R. Ma, C. Zhang, Y. Liu, C. Li, Y. Xu, B. Li, Y. Zhang, Y. An and L. Shi, *RSC Adv.*, 2017, **7**, 21328–21335.
68 A. Biswas, T. Ghosh, P. K. Gavel and A. K. Das, *ACS Appl. Bio Mater.*, 2020, **3**, 1052–1060.
69 R. Cheng, G. Li, L. Fan, J. Jiang and Y. Zhao, *Chem. Commun.*, 2020, **56**, 12246–12249.
70 E. N. Keyzer, A. Sava, T. K. Ronson, J. R. Nitschke and A. J. McConnell, *Chem. – Eur. J.*, 2018, **24**, 12000–12005.
71 P. Harders, T. Griebenow, A. Businski, A. J. Kaus, L. Pietsch, C. Näther and A. J. McConnell, *ChemPlusChem*, 2022, **87**, e202200022.
72 Y. Liu, H. Yi, T. Tao, P. Hoa and C. Chunyan, *Angew. Chem., Int. Ed.*, 2018, **57**, 9023–9027.
73 K. Oda, S. Hiroto and H. Shinokubo, *J. Mater. Chem. C*, 2017, **5**, 5310–5315.
74 A. Wilson, G. Gasparini and S. Matile, *Chem. Soc. Rev.*, 2014, **43**, 1948–1962.
75 M. Gomberg, *J. Am. Chem. Soc.*, 1900, **22**, 757–771.
76 H. D. Hartzler, *J. Org. Chem.*, 1966, **31**, 2654–2658.
77 J. Ohkanda, Y. Mori, K. Maeda and E. Osawa, *J. Chem. Soc., Perkin Trans. 2*, 1992, 59–63.
78 C. Harnack, W. Krull, M. Lehnig, W. P. Neumann and A. K. Zarkadis, *J. Chem. Soc., Perkin Trans. 2*, 1994, 1247–1252.
79 T. Kobashi, D. Sakamaki and S. Seki, *Angew. Chem., Int. Ed.*, 2016, **55**, 8634–8638.
80 M. Frenette, C. Aliaga, E. Font-Sanchis and J. C. Scaiano, *Org. Lett.*, 2004, **6**, 2579–2582.
81 J. P. Peterson, M. R. Geraskina, R. Zhang and A. H. Winter, *J. Org. Chem.*, 2017, **82**, 6497–6501.
82 D. Wang, C. Capel Ferrón, J. Li, S. Gámez-Valenzuela, R. Ponce Ortiz, J. T. López Navarrete, V. Hernández Jolín, X. Yang, M. Peña Álvarez, V. García Baonza, F. Hartl, M. C. Ruiz Delgado and H. Li, *Chem. – Eur. J.*, 2017, **23**, 13776–13783.
83 B. Adinarayana, D. Shimizu, K. Furukawa and A. Osuka, *Chem. Sci.*, 2019, **10**, 6007–6012.
84 K. Imato, A. Irie, T. Kosuge, T. Ohishi, M. Nishihara, A. Takahara and H. Otsuka, *Angew. Chem., Int. Ed.*, 2015, **54**, 6168–6172.
85 W. P. Neumann, A. Penenory, U. Stewen and M. Lehnig, *J. Am. Chem. Soc.*, 1989, **111**, 5845–5851.
86 G. Wittig, E. Dreher, W. Reuther, H. Weidinger and R. Steinmetz, *Justus Liebigs Ann. Chem.*, 1969, **726**, 188–200.
87 D. Beaudoin, O. Levasseur-Grenon, T. Maris and J. D. Wuest, *Angew. Chem., Int. Ed.*, 2016, **55**, 894–898.
88 S. Fukuzumi and J. K. Kochi, *J. Org. Chem.*, 1980, **45**, 2654–2662.
89 C. Ollivier, R. Chuard and P. Renaud, *Synlett*, 1999, 807–809.
90 M. Pouliot, P. Renaud, K. Schenk, A. Studer and T. Vogler, *Angew. Chem., Int. Ed.*, 2009, **48**, 6037–6040.